Interfering pathways in benzene: An analytical treatment

Thorsten Hansen,[a] Gemma C. Solomon, David Q. Andrews, and Mark A. Ratner
Department of Chemistry, Northwestern University, 2145 Sheridan Road, Evanston, Illinois 60208, USA

(Received 17 June 2009; accepted 18 October 2009; published online 18 November 2009)

The mechanism for off-resonant electron transport through small organic molecules in metallic junctions is predominantly coherent tunneling. Thus, new device functionalities based on quantum interference could be developed in the field of molecular electronics. We invoke a partitioning technique to give an analytical treatment of quantum interference in a benzene ring. We interpret the antiresonances in the transmission as either *multipath* zeroes resulting from interfering spatial pathways or *resonance* zeroes analogous to zeroes induced by sidechains. © *2009 American Institute of Physics*. [doi:10.1063/1.3259548]

I. INTRODUCTION

Quantum coherences of exciton transfer processes have been measured in photosynthetic reaction centers, suggesting that quantum mechanical effects may underlie the near-perfect quantum efficiency of photosynthesis.[1,2] Inspired by nature, one could envision molecular electronic devices with functionalities derived from quantum interference.[3–9] This appears feasible, as the dominant mechanism for electron transfer in many molecular transport junctions is coherent transport, and the current is generally well described by the Landauer equation. The coherent transport picture breaks down as the junction approaches resonant transport due to charging and increased electronic-vibrational coupling; consequently, coherent molecular devices should function in the off-resonant regime. Understanding destructive interference features is therefore important for the prospects of molecular electronics as these features can potentially be integrated into designs and manipulated to obtain molecular devices with a large dynamic range.[10–25]

Interference effects in transport through aromatic systems in general, and through benzene in particular, have be studied both experimentally[26,27] and theoretically.[28–38] The large variation in transmission through a benzene ring as the substitution is changed from ortho to meta and to para (shown in Fig. 1) has been attributed to quantum interference. Working with a model Hamiltonian, at the Hückel level of electronic structure, we shall demonstrate how to interpret the negative interference features of the transmission functions for benzene in terms of interfering pathways by which the tunneling electron travels one way and another through the benzene ring. All but one of the antiresonances fit into this interpretation, and we shall make the distinction between *multipath* zeroes and *resonance* zeroes of the transmission function, a distinction that may prove helpful for the design of novel molecular devices.

The quantitative accuracy of contemporary transport calculations, with the electronic structure treated at the density functional theory level, is far superior to the simplistic model calculations used in this work. Yet, we expect the conceptual conclusions of our analytical treatment to carry over to larger numerical calculations, not unlike the computational work of Ke *et al.*,[37] where interference features were not seen in benzene due to strong mixing of the molecular π-system and the σ orbitals of the electrode, but they were evident in larger conjugated rings.

The key mathematical entity in molecular conductance calculations is the molecular Green's function, which is calculated from the molecular Hamiltonian and, possibly, additional self-energies describing interactions with surroundings or additional degrees of freedom. Most computational approaches calculate the transmission via the Green's function. Working at the Hückel level of theory, we are able to give a fully analytical treatment, dissecting the molecular Green's functions using two different theoretical techniques. We invoke a Löwdin partitioning scheme to interpret the antiresonances of the molecular Green's function as the result of interfering spatial pathways. To describe the coupling between the molecule and metallic leads, we use perturbation theory to first order in the self-energy. This will allow us to treat linewidths and the splitting of degenerate orbitals on the imaginary energy axis, which causes dips in the transmission.

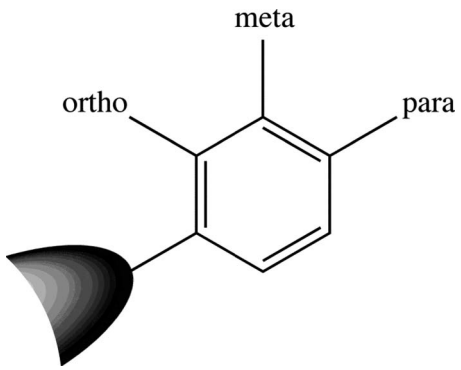

FIG. 1. Three different ways to attach electrodes to benzene.

[a]Author to whom correspondence should be addressed. Electronic mail: thorsten@chem.northwestern.edu.

II. MOLECULAR TRANSMISSION

The rate of electron transfer in molecular donor-bridge-acceptor systems is often described by a generalized Fermi's golden rule,

$$k_{\mathrm{AD}} = \frac{2\pi}{\hbar}\sum_{ad} |t_{ad}(\varepsilon_d)|^2 \delta(\varepsilon_a - \varepsilon_d). \tag{1}$$

Here t_{ad} describes the transition matrix and the sums run over orbitals, with energies ε_d and ε_a, spanning the donor and acceptor components of the molecule, respectively. A definition of the transition matrix is given by

$$t_{ad}(E) = V_{ad} + \sum_{ij} V_{ai} G^{\mathrm{ret}}_{ij}(E) V_{jd}. \tag{2}$$

Here V is the coupling, or perturbation, and $G^{\mathrm{ret}}(E)$ is the retarded Green's function, described below.[39–43] In this work, we assume that the electron transfer is bridge mediated; thus $V_{ad}=0$.

Most contemporary approaches to molecular transport junctions work with the Landauer equation

$$I = \frac{2e}{h}\int dE(f_L(E) - f_R(E))T(E). \tag{3}$$

The transmission function,

$$T(E) = \mathrm{Tr}\{\Gamma^L G^{\mathrm{ret}}(E)\Gamma^R G^{\mathrm{adv}}(E)\}, \tag{4}$$

is the property that is calculated in most computational approaches to molecular electronics.[44–52] The advanced Green's function, $G^{\mathrm{adv}}(E)$, is the Hermitian conjugate of the retarded Green's function described below, $G^{\mathrm{adv}}(E) = (G^{\mathrm{ret}}(E))^{\dagger}$, and Γ^X is the spectral density of the left or right lead, $X=L$ and R and is defined as

$$\Gamma^L_{ij}(E) = 2\pi\sum_d V_{id}V_{dj}\delta(E-\varepsilon_d). \tag{5}$$

To elucidate the analogy between the rate expression (1) and the Landauer equation, we rewrite the transmission as a Fisher–Lee type expression[18,53,54]

$$\begin{aligned} T(E) &= 4\pi^2\sum_{ad}\sum_{ijkl}(V_{ai}G^{\mathrm{ret}}_{ij}(E)V_{jd})(V_{dk}G^{\mathrm{adv}}_{kl}(E)V_{la}) \\ &\quad\times\delta(E-\varepsilon_d)\delta(E-\varepsilon_a) \\ &= 4\pi^2\sum_{ad}|t_{ad}(E)|^2\delta(E-\varepsilon_d)\delta(E-\varepsilon_a). \end{aligned} \tag{6}$$

The rate expression, Eq. (1), is then recovered by integrating over the independent energy variable

$$k_{\mathrm{AD}} = \frac{1}{h}\int dET(E). \tag{7}$$

A. The Green's function

Under quite general conditions we can study the quantum interference phenomena occurring in either photochemical donor-bridge-acceptor systems or molecular transport junctions by focusing on the retarded Green's operator of the bridging molecule, which is defined by

$$G^{\mathrm{ret}}(E) = \frac{1}{E - H + i\eta}. \tag{8}$$

Here H is the Hamiltonian in question, and η is a positive infinitesimal. In the case of donor-bridge-acceptor systems, we take H to be the Hückel Hamiltonian of the molecular bridge. For a molecular transport junction, we will add the coupling to the leads as an imaginary potential. All Green's functions described below will be retarded, so the superscript ret and the imaginary infinitesimal $i\eta$ will be omitted.

Mathematically, we shall adopt two complementary viewpoints when analyzing the Green's functions. From a linear algebra point of view, the retarded Green's operator is a restriction of the resolvent, $G(E)=(E-H)^{-1}$, which is obtained by matrix inversion of the operator $E-H$. A closed expression for a specific matrix element of the resolvent is given as the ratio between the so-called cofactor, $\mathcal{C}_{ji}(E-H)$, and the secular determinant,

$$G_{ij}(E) = \frac{\mathcal{C}_{ji}(E-H)}{\det(E-H)}. \tag{9}$$

The jith cofactor of a matrix A is given as

$$\mathcal{C}_{ji}(A) = (-1)^{j+i}\det(\tilde{A}_{ji}), \tag{10}$$

where $\tilde{A}_{ji}$ is the submatrix of A obtained by removing the jth row and the ith column.

From a complex analysis point of view, we consider the Green's function, Eq. (9), as a function of the (in general complex) energy variable E. It is meromorphic since it is given as the ratio of two polynomials in E. The poles of the Green's function thus coincide with the zeros of the secular determinant, i.e., the eigenenergies of the molecular Hamiltonian.

Likewise, antiresonances in the transmission, where the Green's function and hence the transmission function equal zero, are due to zeroes in the cofactor. However, not all zeroes of the cofactor result in an antiresonance in the transmission. The Hamiltonian H is a simple matrix, i.e., it has a full set of eigenvectors and is thus diagonalizable. A theorem for simple matrices implies that all poles of the Green's function are simple poles; thus any degenerate eigenvalues of H are roots of the cofactor.[55] As we shall see below, the breaking of a degeneracy will therefore make an additional antiresonance appear.

In simple cases, where the Hamiltonian can be diagonalized exactly, it can be helpful to expand the Green's operator in a basis of eigenvectors, $\{|u_i\rangle\}$. We write

$$G(E) = \frac{1}{E-H} = \sum_i \frac{|u_i\rangle\langle u_i|}{E-\varepsilon_i}. \tag{11}$$

Thus the residue of the pole at ε_i is the orthogonal projection onto the eigenvector, $|u_i\rangle\langle u_i|$. The residue of a degenerate eigenvalue is obtained by summation over a full basis for the eigenspace, $\mathrm{res}(\varepsilon_i)=\Sigma_{j;\varepsilon_j=\varepsilon_i}|u_j\rangle\langle u_j|$.

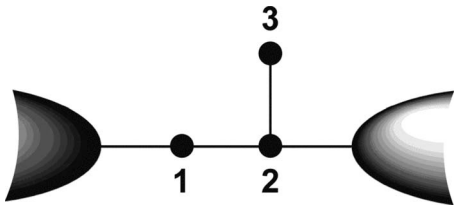

FIG. 2. A three-site model wire.

III. MOLECULAR TOPOLOGY

Only in the simplest cases can we diagonalize the Hückel Hamiltonian exactly and obtain analytical expressions for the eigenenergies and eigenvalues. However, by projecting the full problem onto a small subspace of the full Hilbert space, we obtain an effective Hamiltonian for this smaller space. The parts of the molecule that have been disregarded, e.g., some substituents, are therefore only described indirectly, yet their impact on the subspace in question is described exactly.

The Green's functions of interest for electron transmission are then expressed in terms of the effective Hamiltonian. The parts of the molecule that have been removed will appear as self-energies in the Green's functions, and the mathematical structure of the self-energies will directly reflect the topology of the molecule. In this way we obtain an exact analytical expression for the Green's functions.

A. Löwdin partitioning

First, we shall briefly review the Löwdin partitioning technique.[56–58] Let $P=\Sigma_i|i\rangle\langle i|$ be a projection operator onto the subspace of interest, and let $Q=1-P$ be the projection onto the complementary subspace. Orthogonal projection operators are Hermitian, $P=P^\dagger$, and idempotent, $P^2=P$. We can write the uncoupled Hamiltonian as $H^0=\Sigma_i\alpha|i\rangle\langle i|$; thus the projection operators commute with H^0, $[P,H^0]=[Q,H^0]=0$. Beginning with the definition of the Green's function,

$$(E-H^0-V)G(E)=1, \tag{12}$$

and multiplying on the right with P and on the left with P or Q, we insert $P+Q=1$ and use the commutation relations to obtain

$$P(E-H)P[PG(E)P]-PVQ[QG(E)P]=P, \tag{13}$$

$$-QVP[PG(E)P]+Q(E-H)Q[QG(E)P]=0. \tag{14}$$

From these equations, the projection, $PG(E)P$, of the Green's function can be isolated,

$$PG(E)P=\frac{P}{E-PH^0P-P\Sigma(E)P}. \tag{15}$$

Here $\Sigma(E)$ is a self-energy, or level-shift, operator defined by

$$\Sigma(E)=V+V\frac{Q}{E-QH^0Q-QVQ}V. \tag{16}$$

Note the close analogy to Eq. (2). As an example, consider the three-site Hamiltonian of the system depicted in Fig. 2,

$$H=\begin{bmatrix}\alpha & \beta & 0\\ \beta & \alpha & \beta'\\ 0 & \beta' & \alpha'\end{bmatrix}. \tag{17}$$

Now we remove the sidechain by defining $P=|1\rangle\langle 1|+|2\rangle\langle 2|$. This implies $Q=|3\rangle\langle 3|$, and using Eq. (16), we obtain a self-energy

$$P\Sigma(E)P=PVQ\frac{1}{E-H}QVP=\frac{\beta'^2}{E-\alpha'}|2\rangle\langle 2|, \tag{18}$$

which is introduced in the effective Hamiltonian

$$H^{\text{eff}}=\begin{bmatrix}\alpha & \beta\\ \beta & \alpha+\Sigma(E)\end{bmatrix}. \tag{19}$$

Even though we have reduced the dimension of the Hamiltonian, the self-energy ensures that we obtain the exact result for Green's functions defined in the reduced Hilbert space,

$$\begin{aligned}G_{21}(E)&=\langle 2|\frac{1}{E-H^{\text{eff}}}|1\rangle\\ &=\frac{\beta}{(E-\alpha-\Sigma(E))(E-\alpha)-\beta^2}\\ &=\frac{1}{E-\alpha}\beta\frac{1}{E-\alpha-\Sigma(E)-\dfrac{\beta^2}{E-\alpha}}.\end{aligned} \tag{20}$$

The last expression could be obtained via Dyson's equation, which in this case reads $G_{21}(E)=G^0_{22}(E)\beta G_{11}(E)$. When the energy variable E is resonant with the sidechain energy α', the self-energy diverges. This implies $G_{11}(\alpha')=0$, which offers a characterization of the antiresonances induced by sidechains. A pole in the self-energy implies an antiresonance in the Green's function.[13–21,24]

In molecular electronics, the metal leads bonded to a molecule are also described with the partitioning technique. Often, the so-called wide-band approximation is used, in which case only the resonant part of the self-energy remains, constituting an imaginary potential in the molecular Hamiltonian. This approach is taken in Sec. V.

B. Paths through cyclic systems

The ring topology of any cyclic molecule means that the partitioning technique can be used to describe the transmission in terms of different spatial paths around the ring. For example, in benzene the self-energy terms appearing in the effective Hamiltonian $H^{\text{eff}}(E)$ can be assigned to one of two distinct spatial paths, A or B, between sites $|a\rangle$ and $|b\rangle$, as shown in Fig. 3,

$$H^{\text{eff}}(E)=\begin{bmatrix}\alpha+\Sigma^A_{aa}+\Sigma^B_{aa} & \Sigma^A_{ab}+\Sigma^B_{ab}\\ \Sigma^A_{ba}+\Sigma^B_{ba} & \alpha+\Sigma^A_{bb}+\Sigma^B_{bb}\end{bmatrix}. \tag{21}$$

The Hamiltonian $H^{\text{ret}}(E)$ is symmetric since $\Sigma^X_{ab}=\Sigma^X_{ba}$ for $X=A,B$.

If we consider the diagonal part of this effective Hamiltonian as the unperturbed Hamiltonian and the off-diagonal

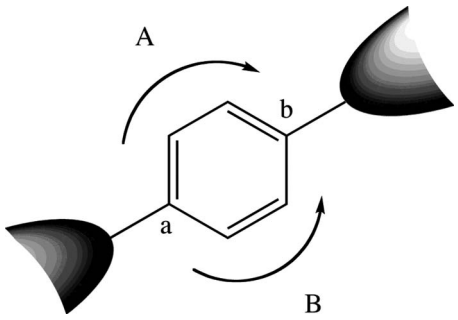

FIG. 3. Two pathways through benzene; in this case, para.

elements as the perturbation, we can use Dyson's equation to write the off-diagonal element of the Green's function $G_{ba}(E)$ as

$$G_{ba}(E) = \frac{1}{E-\alpha-\Sigma^A_{bb}-\Sigma^B_{bb}-\dfrac{(\Sigma^A_{ba}+\Sigma^B_{ba})(\Sigma^A_{ab}+\Sigma^B_{ab})}{E-\alpha-\Sigma^A_{aa}-\Sigma^B_{aa}}} \times(\Sigma^A_{ba}+\Sigma^B_{ba})\frac{1}{E-\alpha-\Sigma^A_{aa}-\Sigma^B_{aa}}. \quad (22)$$

This expression takes the form $G_{bb}(E)\Sigma_{ba}(E)G^0_{aa}(E)$, where the three factors give the contributions from site $|b\rangle$, the two paths, and site $|a\rangle$, respectively. The first factor, $G_{bb}(E)$, is the full Green's function for the site $|b\rangle$, with self-energies describing virtual excursions into the bridges, Σ^A_{bb} and Σ^B_{bb}, and to the site $|a\rangle$ and back, $(\Sigma^A_{ba}+\Sigma^B_{ba})(\Sigma^A_{ab}+\Sigma^B_{ab})/(E-\alpha-\Sigma^A_{aa}-\Sigma^B_{aa})$. Note that the two distinct paths lead to $2^2=4$ similar terms in the self-energy. The last factor is the uncoupled Green's function for the site $|a\rangle$, with self-energies describing virtual excursions into the bridges A and B.

There are two conditions that will cause the Green's function to have a zero and thus an antiresonance in the transmission. Either the sum of the self-energies, $\Sigma^A+\Sigma^B$, is zero or the product $G_{bb}(E)G^0_{aa}(E)$ is zero because of a pole in one of the self-energies, Σ^A or Σ^B. We will refer to the former as multipath zeroes because they occur when the self-energies of the two paths around the ring cancel each other. We will refer to the latter as resonance zeroes because they occur when the energy variable E is resonant with an eigenenergy of the substructure of the molecule described by the self-energy. This is directly analogous to the zeroes caused by sidechains, as described above.

In the terminology of the renormalized perturbation expansion,[59,60] used, e.g., to describe electron transfer in proteins,[41] multipath zeroes are the result of interference of two or more skeleton paths. Resonance zeroes, on the other hand, result from a decoration that all skeletons paths have in common.

C. Cofactor factorization theorem

We now have two ways of characterizing the zeroes of the Green's function and thus the antiresonances of the transmission function. On the one hand, zeroes of the Green's function are zeroes of the cofactor, as seen from Eq. (9). On the other hand, from the discussion of Eq. (22), zeroes of the Green's function are either multipath zeroes, meaning zeroes of the sum of self-energies $\Sigma^A+\Sigma^B$, or resonance zeroes, where either Σ^A or Σ^B is divergent. We can elucidate the connection with a factorization theorem for the cofactor.

In the simple case, when the Hamiltonian is reduced to two dimensions, say, $P=|1\rangle\langle 1|+|2\rangle\langle 2|$, the off-diagonal cofactors that we are interested in can be factorized as:

$$\mathcal{C}_{12}(E-H) = \det(Q(E-H)Q)\langle 2|\Sigma(E)|1\rangle. \quad (23)$$

To derive this result, we begin with the definition of the cofactor from Eq. (9),

$$\mathcal{C}_{12}(E-H) = \det(E-H)\langle 2|(E)|1\rangle. \quad (24)$$

With the projection operators P and Q, we can write the Hamiltonian as a block matrix,

$$H = \begin{bmatrix} PHP & PHQ \\ QHP & QHQ \end{bmatrix}, \quad (25)$$

and use a standard identity for the determinant of a block matrix to obtain

$$\det(E-H) = \det(Q(E-H)Q)\det(E-PH^0P-P\Sigma(E)P). \quad (26)$$

Defining $H^{\text{eff}}=PH^0P+P\Sigma(E)P$, we can now write Eq. (24) as

$$\mathcal{C}_{12}(E-H) = \det(Q(E-H)Q)\det(E-H^{\text{eff}})\langle 2|\frac{1}{E-H^{\text{eff}}}|1\rangle \quad (27)$$

$$= \det(Q(E-H)Q)\mathcal{C}_{12}(E-H^{\text{eff}}). \quad (28)$$

When H^{eff} is a two by two matrix, we have $\mathcal{C}_{12}(E-H^{\text{eff}})=\langle 2|\Sigma(E)|1\rangle$, which completes the proof. Thus multipath zeroes are zeroes of the self-energy $\langle 2|\Sigma(E)|1\rangle$, whereas resonance zeroes are zeroes of the determinant $\det(Q(E-H)Q)$. We shall use this factorization below when discussing the ortho, meta, and para cofactors of benzene.

IV. UNDERSTANDING BENZENE

We now apply these methods to study the transport through the prototypical cyclic system: benzene. A Hückel Hamiltonian for the π system of benzene can be written as

$$H = \sum_{i=1}^{6}\alpha|i\rangle\langle i| + \sum_{i=1}^{6}\beta(|i\rangle\langle i+1| + |i+1\rangle\langle i|), \quad (29)$$

where $|i\rangle$ represents the p-orbital on atom i, and we define $|7\rangle\equiv|1\rangle$ to describe the ring topology. The different substitution patterns result from coupling different sites to the electrodes, sites $|1\rangle$ and $|2\rangle$, $|1\rangle$ and $|3\rangle$, and $|1\rangle$ and $|4\rangle$ for ortho, meta, and para, respectively.

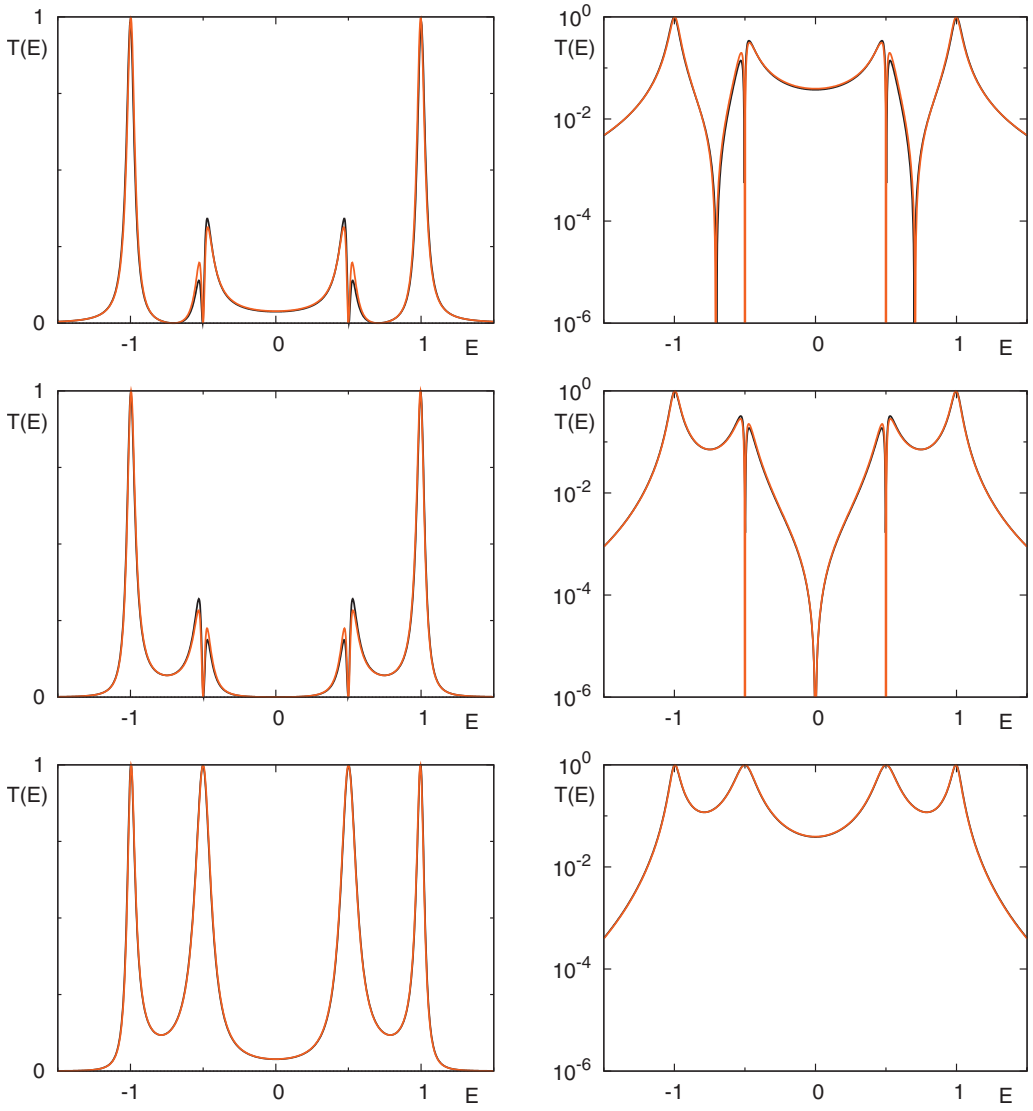

FIG. 4. Transmission function $T(E)$ for the ortho (top), meta (middle), and para (bottom) systems. $\alpha=0$, $\beta=-0.5$, and $\Gamma=0.2$. Linear scale on the left and logarithmic scale on the right. In all cases both the exact solution (red) and a simplified perturbative treatment of the electrodes (black) as outlined in Sec. V are shown.

These changes in the substitution pattern result in dramatically different transmissions through the system. Figure 4 illustrates the different transmissions on both linear and logarithmic scales. The differences in the resonances can be seen clearly on the linear scale and, in particular, the dramatic differences in the antiresonances on the logarithmic scale.

The relevant energy range for chemical reactivity is between the highest occupied and the lowest unoccupied molecular orbitals. In this entire range the transmission in the meta case is largely suppressed due to the antiresonance at zero. This is fully consistent with the rules for electrophilic substitution reactions on benzene; the ortho and para positions are electron rich or deficient depending on whether the first substituent is electron donating or withdrawing. The meta position, on the other hand, has no coupling to the first substituent due to the suppression of the transmission function.[61] Now we apply the techniques developed previously to see how these differences arise from the properties of the Green's function.

A. Constructing the Green's function

The Hückel Hamiltonian of benzene can be diagonalized exactly, and we take advantage of this to calculate explicit expressions for the Green's functions by using Eq. (11). Whereas the results from the previous section do not require diagonalization and are thus applicable to all molecules, knowledge of the eigenenergies and molecular orbitals of benzene enables us to give a more explicit and detailed analysis of our case study. The eigenvalues are $\alpha+2\beta$, $\alpha+\beta$, $\alpha-\beta$, and $\alpha-2\beta$, and the secular determinant factorizes as

$$\det(E-H)=(E-\alpha-2\beta)(E-\alpha-\beta)^2(E-\alpha+\beta)^2 \times(E-\alpha+2\beta). \tag{30}$$

We construct a unitary matrix U by writing a set of normalized eigenvectors $\{|u_i\rangle\}$ as columns,

TABLE I. Residues in the ortho, meta, and para cases.

	$G_{ij}(E)$	$\alpha+2\beta$	$\alpha+\beta$	$\alpha-\beta$	$\alpha-2\beta$
Ortho	$G_{21}(E)$	$\frac{1}{6}$	$\frac{1}{6}$	$-\frac{1}{6}$	$-\frac{1}{6}$
Meta	$G_{31}(E)$	$\frac{1}{6}$	$-\frac{1}{6}$	$-\frac{1}{6}$	$\frac{1}{6}$
Para	$G_{41}(E)$	$\frac{1}{6}$	$-\frac{1}{3}$	$\frac{1}{3}$	$-\frac{1}{6}$

$$U=\frac{1}{\sqrt{6}}\begin{bmatrix} 1 & -\frac{1}{\sqrt{2}} & \sqrt{\frac{3}{2}} & -\frac{1}{\sqrt{2}} & -\sqrt{\frac{3}{2}} & -1 \\ 1 & -\sqrt{2} & 0 & \sqrt{2} & 0 & 1 \\ 1 & -\frac{1}{\sqrt{2}} & -\sqrt{\frac{3}{2}} & -\frac{1}{\sqrt{2}} & \sqrt{\frac{3}{2}} & -1 \\ 1 & \frac{1}{\sqrt{2}} & -\sqrt{\frac{3}{2}} & -\frac{1}{\sqrt{2}} & -\sqrt{\frac{3}{2}} & 1 \\ 1 & \sqrt{2} & 0 & \sqrt{2} & 0 & -1 \\ 1 & \frac{1}{\sqrt{2}} & \sqrt{\frac{3}{2}} & -\frac{1}{\sqrt{2}} & \sqrt{\frac{3}{2}} & 1 \end{bmatrix}. \quad (31)$$

When donor and acceptor entities, or two electrodes, are attached to a benzene molecule in either ortho, meta, or para configurations, different matrix elements of the Green's operator, Eq. (11), are relevant. In the ortho case the attachments are to adjacent atoms, e.g., $|1\rangle$ and $|2\rangle$, and we choose to calculate $G_{21}(E)=\langle 2|G(E)|1\rangle$ as

$$G_{21}(E)=\sum_i \frac{\langle 2|u_i\rangle\langle u_i|1\rangle}{E-\varepsilon_i} \quad (32)$$

$$=\frac{1}{6}\frac{1}{E-\alpha-2\beta}+\frac{1}{6}\frac{1}{E-\alpha-\beta}-\frac{1}{6}\frac{1}{E-\alpha+\beta}$$
$$-\frac{1}{6}\frac{1}{E-\alpha+2\beta}. \quad (33)$$

The residues for the ortho, meta, and para Green's function elements are tabulated in Table I. Each residue is a matrix element of an off-diagonal projection operator, which is why the sum of residues in each case is zero. Note also that the ortho and para Green's functions are even functions of energy, $G_{21}(E-\alpha)=G_{21}(-E+\alpha)$, whereas the meta matrix element is an odd function of energy, $G_{31}(E-\alpha)=-G_{31}(-E+\alpha)$; thus the meta matrix element will have a zero, an antiresonance, at $E=\alpha$. These symmetries derive from Coulson's pairing theorem, which ensures a symmetric Hückel spectrum for alternant hydrocarbons.[62] In graph theory, these are the molecules that can be represented by bipartite, or two-color, graphs.[63] After calculating the Green's functions exactly, we now turn to a detailed analysis, in terms of different pathways, for each substitution pattern.

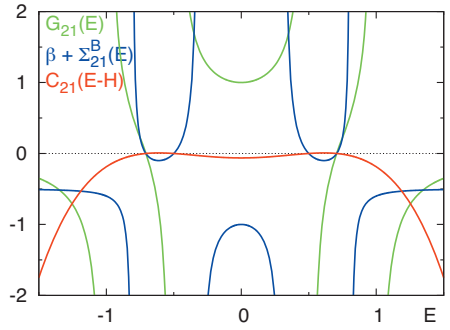

FIG. 5. For ortho substitution, the Green's function (green), $\beta+\Sigma_{21}^{B}(E)$ (blue), and cofactor (red).

1. Ortho

First, we identify the paths through the molecule. In ortho substituted benzene one pathway is the direct bond between the two atoms; thus $\Sigma_{21}^{A}=\beta$ and $\Sigma_{11}^{A}=\Sigma_{22}^{A}=0$, as there are no intervening sites. The second pathway consists of four sites and has the Hückel spectrum of butadiene. The eigenenergies are $\alpha+\phi\beta,\alpha+\beta/\phi,\alpha-\beta/\phi,\alpha-\phi\beta$, where $\phi=(1+\sqrt{5})/2=1.618\ldots$ is the golden ratio and $1/\phi=0.618\ldots=\phi-1$. A set of eigenvectors is given by $\{(c_1,c_2,c_2,c_1),(c_2,c_1,-c_1,-c_2),(c_2,-c_1,-c_1,c_2),(c_1,-c_2,c_2,-c_1)\}$, where $c_1=1/(\sqrt{2}\sqrt{2+\phi})$ and $c_2=\phi c_1$. The off-diagonal self-energy is given as

$$\Sigma_{21}^{B}(E)=\frac{c_1^2\beta^2}{E-\alpha-\phi\beta}-\frac{c_2^2\beta^2}{E-\alpha-\frac{\beta}{\phi}}+\frac{c_2^2\beta^2}{E-\alpha+\frac{\beta}{\phi}}$$
$$-\frac{c_1^2\beta^2}{E-\alpha+\phi\beta}. \quad (34)$$

The diagonal self-energy $\Sigma_{11}^{B}=\Sigma_{22}^{B}$ is given by a similar expression, except that all residues are positive.

The ortho cofactor can now be expressed as the product of the sum of the self-energies of the paths, $\beta+\Sigma_{21}^{B}(E)$, and the secular determinant of the Hückel Hamiltonian for butadiene,

$$\mathcal{C}_{12}(E-H)=(\beta+\Sigma_{21}^{B})\det(Q(E-H)Q)$$
$$=\beta((E-\alpha)^2-\beta^2)((E-\alpha)^2-2\beta^2). \quad (35)$$

Figure 5 shows the Green's function, the sum of the self-energies, and the cofactor plotted as functions of energy.

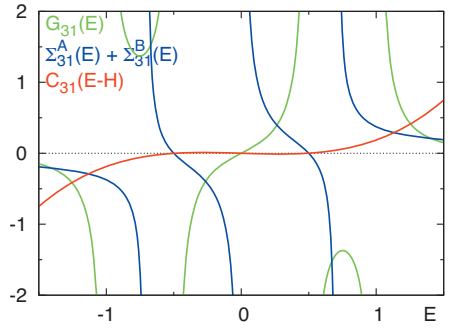

FIG. 6. For meta substitution, the Green's function (green), $\Sigma_{31}^{A}(E)+\Sigma_{31}^{B}(E)$ (blue), and cofactor (red).

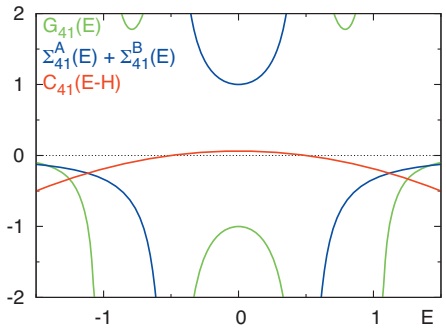

FIG. 7. For para substitution, the Green's function (green), $\Sigma^A_{41}(E)+\Sigma^B_{41}(E)$ (blue), and cofactor (red).

The cofactor is a fourth order polynomial in E and has four real roots. As mentioned above, there will always be roots at the degenerate eigenvalues, in this case $\alpha \pm \beta$, to ensure that these poles of the Green's function are simple poles. As we shall see below, the zeroes at $\alpha \pm \beta$ will manifest themselves when the degeneracy of the eigenvalues is lifted. The two other roots of the cofactor, at $\alpha \pm \sqrt{2}\beta$, cause the Green's function to have zeroes.

The sum of the self-energies for each path, $\beta+\Sigma^B_{21}(E)$, has the four zeroes in common with the cofactor, and we call them multipath zeroes by the distinction made above. Thus the idea of interfering pathways can explain all features of ortho substituted benzene.

2. Meta

In meta substituted benzene the shorter path comprises a single site; thus $\Sigma^A_{31}=\Sigma^A_{11}=\Sigma^A_{33}=\beta^2/(E-\alpha)$. The longer path consists of three sites and has the Hückel spectrum of propene, with eigenvalues $\alpha+\sqrt{2}\beta, \alpha, \alpha-\sqrt{2}\beta$. A set of eigenvectors is given by $\{(1/2, 1/\sqrt{2}, 1/2), (1/\sqrt{2}, 0, -1/\sqrt{2}), (1/2, -1/\sqrt{2}, 1/2)\}$. The off-diagonal self-energy is given as

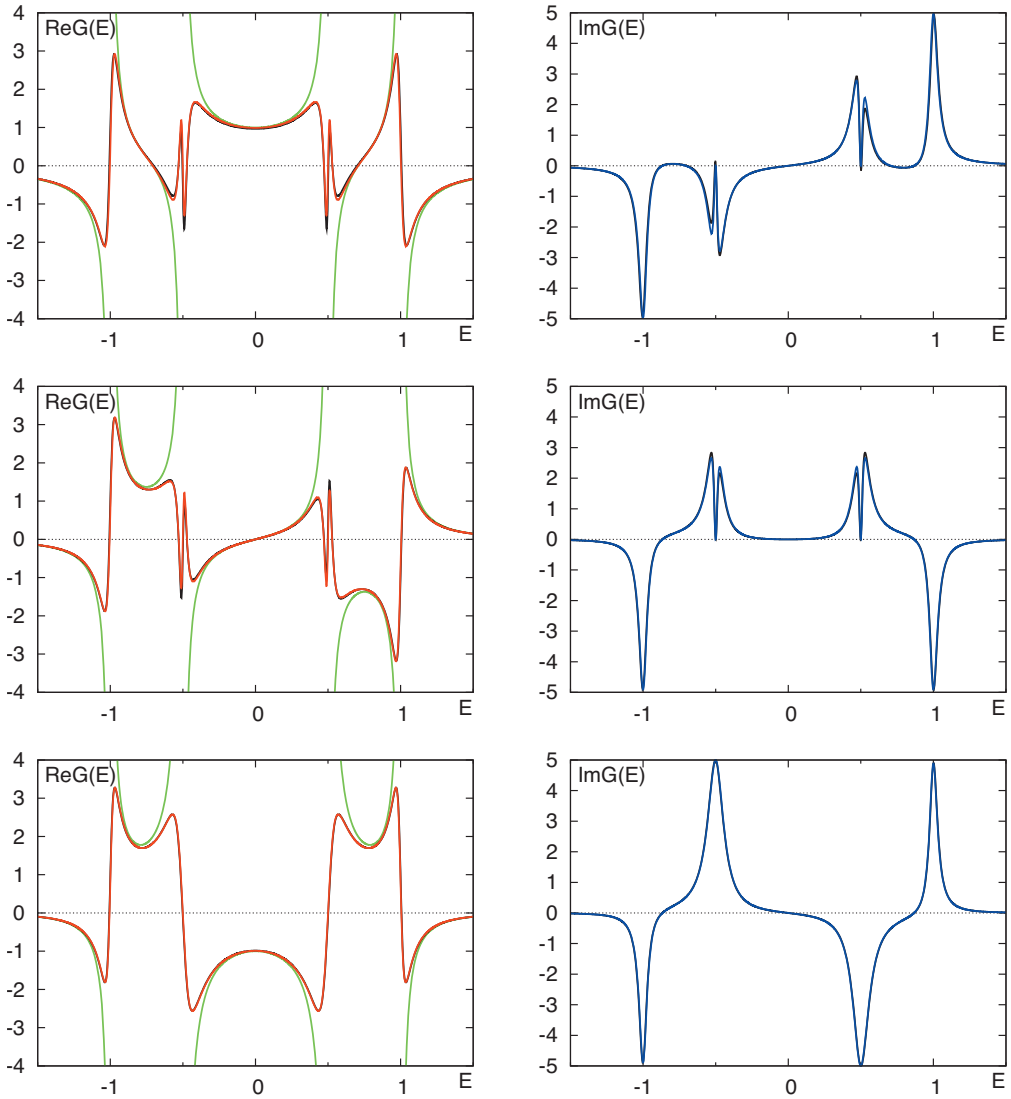

FIG. 8. The real (left) and imaginary (right) parts of the Green's functions for (from top to bottom) ortho, meta, and para substitution patterns. Left: the real part Re $G(E)$ for the uncoupled system (green), the coupled system calculated exactly (red), and the coupled system calculated by first order perturbation in Γ (black). Right: the imaginary part Im $G(E)$ for the coupled system calculated exactly (blue) and the first order perturbation in Γ (black). For all plots: $\alpha=0$, $\beta=-0.5$, and $\Gamma=0.2$.

$$\Sigma_{31}^{B}(E) = \frac{\beta^2}{4}\frac{1}{E-\alpha-\sqrt{2}\beta} - \frac{\beta^2}{2}\frac{1}{E-\alpha} + \frac{\beta^2}{4}\frac{1}{E-\alpha+\sqrt{2}\beta}. \tag{36}$$

The diagonal self-energy $\Sigma_{11}^{B}=\Sigma_{33}^{B}$ is given by a similar expression, except that all residues are positive. The cofactor is given as the sum of the self-energies, $\Sigma_{31}^{A}(E)+\Sigma_{31}^{B}(E)$, times the secular determinant of the paths,

$$\begin{aligned}\mathcal{C}_{13}(E-H) &= (\Sigma_{31}^{A}(E)+\Sigma_{31}^{B}(E))\det(Q(E-H)Q)\\ &= \beta^2(E-\alpha)((E-\alpha)^2-\beta^2).\end{aligned} \tag{37}$$

Figure 6 shows the Green's function, the sum of the self-energies, and the cofactor plotted as functions of energy. The cofactor is a third order polynomial in E and has three real roots. As mentioned above, there will always be roots at the degenerate eigenvalues, in this case $\alpha\pm\beta$, to ensure that these poles of the Green's function are simple poles. The third root causes the Green's function to have a zero at $E=\alpha$.

The sum of the self-energies, $\Sigma_{31}^{A}(E)+\Sigma_{31}^{B}(E)$, has two zeroes in common with the cofactor ($E=\alpha\pm\beta$). Again, these are multipath zeroes, which will manifest themselves when the eigenvalue degeneracy is lifted. Notably, the third zero, at $E=\alpha$, cannot be thought of as resulting from interfering pathways. We call it a resonance zero and emphasize that it is analogous to zeroes induced by sidechains in a molecular structure, a fact that should be considered when designing molecules for interference experiments since the zero is at $E=\alpha$ and thus will be near the Fermi level in experimental realizations.

3. Para

For para substitution, the two paths are identical and each consists of two sites. The eigenvalues are $\alpha\pm\beta$ with bonding and nonbonding eigenvectors $\{(1/\sqrt{2},1/\sqrt{2}),(1/\sqrt{2},-1/\sqrt{2})\}$. The off-diagonal self-energy is given by

$$\Sigma_{41}^{A}(E) = \Sigma_{41}^{B}(E) = \frac{\beta^2}{2}\frac{1}{E-\alpha-\beta} - \frac{\beta^2}{2}\frac{1}{E-\alpha+\beta}. \tag{38}$$

Each diagonal self-energy is given by a similar expression with both residues positive. The cofactor is given as the product of the sum of the self-energies and the secular determinants of the paths,

$$\begin{aligned}\mathcal{C}_{14}(E-H) &= (\Sigma_{41}^{A}(E)+\Sigma_{41}^{B}(E))((E-\alpha)^2-\beta^2)^2\\ &= 2\beta^3((E-\alpha)^2-\beta^2).\end{aligned} \tag{39}$$

Figure 7 shows the Green's function, the sum of the self-energies, and the cofactor, plotted as a function of energy. The cofactor is a second order polynomial in E and has two real roots. These are located at the degenerate eigenvalues $\alpha\pm\beta$ as described above. These zeroes are provided by the secular determinant and are therefore resonance zeroes. As we shall discuss below, they will not, for symmetry reasons, manifest themselves in the transmission function when the degeneracies are lifted.

V. LINEWIDTHS

Until now, we have focused on the Green's function derived from the Hamiltonian of the isolated molecule. As the molecule couples to the two metal electrodes, the molecular levels broaden and the resonances in the transmission function acquire width. A self-energy in the molecular Hamiltonian captures this. The imaginary part of the self-energy describes the broadening, whereas the real part shifts the energy levels. We work in the wide-band approximation where the self-energy is purely imaginary. For each atomic site that couples to an electrode, we shift the energy as

$$\alpha \to \alpha - i\frac{\Gamma}{2}. \tag{40}$$

The spectral density is denoted Γ. The sign of the energy shift is negative because we work with retarded Green's functions.

We focus on the atomic sites, say, $\{|a\rangle,|b\rangle\}$, that are coupled directly to the electrodes. Using the Löwdin partitioning to project onto the Hilbert space that they span, we obtain an effective Hamiltonian, which for our test case of benzene reads

$$H^{\text{eff}}(E) = \begin{bmatrix} \alpha - i\dfrac{\Gamma}{2} + \Sigma_{aa}^{A} + \Sigma_{aa}^{B} & \Sigma_{ab}^{A} + \Sigma_{ab}^{B} \\ \Sigma_{ba}^{A} + \Sigma_{ba}^{B} & \alpha - i\dfrac{\Gamma}{2} + \Sigma_{bb}^{A} + \Sigma_{bb}^{B} \end{bmatrix}, \tag{41}$$

where A and B, as above, denote the two pathways through benzene. For a 2×2 Hamiltonian, the resolvent can be obtained analytically, and the $G_{ba}(E)$ element reads

$$G_{ba}(E) = \frac{\Sigma_{ba}^{A}+\Sigma_{ba}^{B}}{\left(E-\alpha+i\dfrac{\Gamma}{2}-\Sigma_{aa}^{A}-\Sigma_{aa}^{B}\right)\left(E-\alpha+i\dfrac{\Gamma}{2}-\Sigma_{bb}^{A}-\Sigma_{bb}^{B}\right)-(\Sigma_{ab}^{A}+\Sigma_{ab}^{B})(\Sigma_{ba}^{A}+\Sigma_{ba}^{B})}. \tag{42}$$

This expression is exact and it requires no knowledge of eigenvalues or eigenvectors. We use it when plotting the Green's functions and transmission functions.

Since the perturbation is imaginary, the perturbed Hamil-

tonian is no longer Hermitian, and the residue of a given pole, at ε_i', is no longer the matrix element of an orthogonal projection, $|u_i'\rangle\langle u_i'|$, as in Eq. (11). A general expression is given by

$$G_{ba}(E) = \langle b| \sum_i \frac{|u_i'\rangle\langle v_i'|}{E - \varepsilon_i'} |a\rangle, \tag{43}$$

where $|v_i'\rangle$ is a left eigenvector of the Hamiltonian $\langle v_i'|H = \langle v_i'|\varepsilon_i'$. The perturbed Hamiltonians that we consider are complex symmetric matrices, which implies that any left eigenvector is the complex conjugate of the corresponding right eigenvector $|v_i'\rangle = |\overline{u_i'}\rangle$, and we can construct the Green's function as

$$G_{ba}(E) = \langle b| \sum_i \frac{|u_i'\rangle\langle \overline{u_i'}|}{E - \varepsilon_i'} |a\rangle. \tag{44}$$

The details of calculating the Green's functions for ortho, meta, and para substitutions are given in the Appendix. Both the perturbed and exact Green's functions are shown in Fig. 8. Overall, the first order perturbation expression is in good agreement with the exact result, the largest discrepancies are around the degenerate eigenvalues at $\pm\beta$. With our choice of parameters, the ratio Γ/β equals -0.4. For a β that reproduces the gap between the highest occupied molecular orbital and lowest unoccupied molecular orbital of benzene ($\sim$10 eV), this corresponds to a spectral density of $\sim$2 eV. An experimental spectral density Γ of the order of 1 eV is very large, and we thus conclude that the first order perturbation employed here is a sensible approach.

The Green's functions calculated to first order in Γ are given by

$$G_{43}^{\text{ortho}}(E) = \frac{1}{6}\frac{R_1^o}{E-\alpha-2\beta+i\Gamma/6} - \frac{1}{12}\frac{R_2^o}{E-\alpha-\beta+i\Gamma/12} + \frac{1}{4}\frac{R_3^o}{E-\alpha-\beta+i\Gamma/4} + \frac{1}{12}\frac{R_4^o}{E-\alpha+\beta+i\Gamma/12} - \frac{1}{4}\frac{R_5^o}{E-\alpha+\beta+i\Gamma/4} - \frac{1}{6}\frac{R_6^o}{E-\alpha+2\beta+i\Gamma/6}, \tag{45}$$

$$G_{31}^{\text{meta}}(E) = \frac{1}{6}\frac{R_1^m}{E-\alpha-2\beta+i\Gamma/6} + \frac{1}{12}\frac{R_2^m}{E-\alpha-\beta+i\Gamma/12} - \frac{1}{4}\frac{R_3^m}{E-\alpha-\beta+i\Gamma/4} + \frac{1}{12}\frac{R_4^m}{E-\alpha+\beta+i\Gamma/12} - \frac{1}{4}\frac{R_5^m}{E-\alpha+\beta+i\Gamma/4} + \frac{1}{6}\frac{R_6^m}{E-\alpha+2\beta+i\Gamma/6}, \tag{46}$$

TABLE II. Ortho case. Perturbed eigenvalues and eigenvectors and the residues of the poles of the Green's function.

i	$\varepsilon_i^{(1)}$	Eigenvectors, $\lvert u_i^{(1)}\rangle$	Residue
1	$\alpha+2\beta-i\frac{\Gamma}{6}$	$N_o\left(\lvert u_1\rangle + i\gamma\sqrt{6}\lvert u_3\rangle + i\gamma\frac{\sqrt{2}}{3}\lvert u_4\rangle\right)$	$\frac{1}{6}R_1^o$
2	$\alpha+\beta-i\frac{\Gamma}{12}$	$N_{o''}\left(\lvert u_2\rangle - i\gamma\frac{\sqrt{2}}{3}\lvert u_6\rangle + i\gamma\frac{\sqrt{3}}{2}\lvert u_5\rangle\right)$	$-\frac{1}{12}R_2^o$
3	$\alpha+\beta-i\frac{\Gamma}{4}$	$N_{o'}\left(\lvert u_3\rangle - i\gamma\sqrt{6}\lvert u_1\rangle - i\gamma\frac{\sqrt{3}}{2}\lvert u_4\rangle\right)$	$\frac{1}{4}R_3^o$
4	$\alpha-\beta-i\frac{\Gamma}{12}$	$N_{o''}\left(\lvert u_4\rangle - i\gamma\frac{\sqrt{2}}{3}\lvert u_1\rangle + i\gamma\frac{\sqrt{3}}{2}\lvert u_3\rangle\right)$	$\frac{1}{12}R_4^o$
5	$\alpha-\beta-i\frac{\Gamma}{4}$	$N_{o'}\left(\lvert u_5\rangle + i\gamma\sqrt{6}\lvert u_6\rangle - i\gamma\frac{\sqrt{3}}{2}\lvert u_2\rangle\right)$	$-\frac{1}{4}R_5^o$
6	$\alpha-2\beta-i\frac{\Gamma}{6}$	$N_o\left(\lvert u_6\rangle - i\gamma\sqrt{6}\lvert u_5\rangle + i\gamma\frac{\sqrt{2}}{3}\lvert u_2\rangle\right)$	$-\frac{1}{6}R_6^o$

$$G_{52}^{\text{para}}(E) = \frac{1}{6}\frac{R_1^p}{E-\alpha-2\beta+i\Gamma/6} - \frac{1}{3}\frac{R_2^p}{E-\alpha-\beta+i\Gamma/3} + \frac{1}{3}\frac{R_4^p}{E-\alpha+\beta+i\Gamma/3} - \frac{1}{6}\frac{R_6^p}{E-\alpha+2\beta+i\Gamma/6}. \tag{47}$$

The numerical factors R_i^x $(x=o,m,p)$ have the property that $R_i^x \to 1$ for $\gamma=\Gamma/(12\beta)\to 0$.

The transmission functions, $T(E)=\Gamma^2|G(E)|^2$, are depicted in Fig. 4. In all three cases the widths of the lines at $\alpha\pm 2\beta$, say, Γ', are given by the shift in the poles, $\Gamma'/2 = \Gamma/6 \Rightarrow \Gamma' = \Gamma/3$. No simple notion of linewidth applies to the split peaks at $\alpha\pm\beta$ in the ortho and meta cases. They are dominated by the no longer degenerate levels, whose perturbed energies are split on the imaginary energy axis, which is why the antiresonances at $\alpha\pm\beta$ appear. The slight asymmetry of the lineshapes that is exaggerated by the perturbative treatment stems from the imaginary parts of the eigenvectors. In the para case the width of the resonances at $\alpha\pm\beta$ equals $2\Gamma/3$.

VI. CONCLUSION

In an attempt to open the black box of quantum transport calculations, we have given a fully analytical model treatment of molecular transmission. We have endeavored to probe the relationship between transmission features, electronic structure, and chemical understanding. Quite generally, the Green's functions derived from a Hückel Hamiltonian can be expressed as the ratio of the so-called cofactor over the secular determinant. The presence of the secular determinant in the denominator reiterates the known result that the poles in the Green's function coincide with the molecular orbital energies. Using the Löwdin partitioning technique, we have derived a Dyson's equation for the Green's functions of cyclic molecules. This in turn leads to a factorization theorem for the cofactor, which we have used to distinguish between two types of zeroes of the Green's functions: multipath zeroes, which are a result of the interference of the different spatial pathways through benzene, and reso-

TABLE III. The normalization factors.

Ortho	Meta	Para
$N_o = \left(1 + \frac{56}{9}\gamma^2\right)^{-1/2}$	$N_m = \left(1 + \frac{89}{36}\gamma^2\right)^{-1/2}$	$N_p = \left(1 + \frac{8}{9}\gamma^2\right)^{-1/2}$
$N_{o'} = \left(1 + \frac{27}{4}\gamma^2\right)^{-1/2}$	$N_{m'} = \left(1 + \frac{9}{4}\gamma^2\right)^{-1/2}$	
$N_{o''} = \left(1 + \frac{35}{36}\gamma^2\right)^{-1/2}$		

nance zeroes, which are a result of the tunneling electron being resonant with a substructure of the molecule. Antiresonances induced by sidechains fit into the second category. For a simple yet important example molecule, benzene, we have given a detailed analysis of the interference patterns seen in the transmission functions for the different substitution patterns: ortho, meta, and para.

Some would argue, and rightfully so, that any distinction between different flavors of zeroes is somewhat arbitrary. If the benzene molecule of our analysis is embedded into a larger molecule, the multipath zeroes of the benzene ring will appear as resonance zeroes of this larger molecule. However, we believe that the distinction provides valuable insights into the interference patterns of benzene and could be a useful tool when developing a better chemical understanding of quantum interference in molecules. In fact, the distinction emphasizes the strong analogy to the different resonator designs used in meso- and macroscopic systems: double-slit or stub resonators.

To account for the coupling of the metal electrodes we introduced using perturbation theory an imaginary potential. This caused the transmission resonances to broaden. We calculated the eigenenergies and eigenvectors to first order in the perturbation. The linewidths of the resonances are given by the imaginary shift in energy. In the ortho and meta cases, the degenerate eigenstates are split on the imaginary axis, which allows the hidden multipath zeroes to emerge.

In conclusion, we emphasize the usefulness of analytical techniques, such as Löwdin partitioning and perturbation theory, in analyzing interference in molecular wires. We recommend their use for larger model systems than benzene. Furthermore, we speculate that the application of Löwdin partitioning schemes within the current approach to quantum transport calculations could provide valuable insights into the chemical properties of molecular transport junctions.

ACKNOWLEDGMENTS

T.H. thanks Dr. Paul Sherratt for helpful discussions. T.H. thanks the Carlsberg Foundation (Carlsbergfondet) for support. We thank the MURI program of the DoD, the NCN and MRSEC programs of the NSF, and the ONR and NSF Chemistry divisions for support.

APPENDIX: PERTURBATIVE EIGENVALUES AND EIGENVECTORS

Here we consider the coupling to the electrodes as a perturbation and calculate the poles and residues of the Green's functions to first order in Γ. Remember that the first order correction to an eigenenergy ε_i is simply the expectation value of the perturbation V. We write the perturbed eigenvalue $\varepsilon_i^{(1)}$ as

$$\varepsilon_i^{(1)} = \varepsilon_i + \langle u_i | V | u_i \rangle. \tag{A1}$$

The corresponding perturbed eigenvector is given by

$$|u_i^{(1)}\rangle \propto |u_i\rangle + \sum_{j \neq i} \frac{|u_j\rangle\langle u_j|}{\varepsilon_i - \varepsilon_j} V |u_i\rangle, \tag{A2}$$

which can then be normalized. From the perturbed eigenvalues and eigenvectors, we construct the Green's function.

In the ortho case the two electrodes bind to neighboring sites. One could choose sites $|1\rangle$ and $|2\rangle$, but to take advantage of the eigenvector symmetry, we choose $|3\rangle$ and $|4\rangle$. The perturbation operator in the ortho case now reads

$$V^{\text{ortho}} = -i\frac{\Gamma}{2}(|3\rangle\langle 3| + |4\rangle\langle 4|). \tag{A3}$$

When the perturbation is rotated to the molecular orbital (MO) basis, $V^o = U^{-1} V^{\text{ortho}} U$, it becomes block-diagonal due to our choice of sites. The three molecular orbitals that are even with respect to the symmetry plane of V^{ortho}, namely, $\{|u_1\rangle, |u_3\rangle, |u_4\rangle\}$, mix under the even submatrix,

$$V^o_{\text{even}} = -i\frac{\Gamma}{2}\frac{1}{6}\begin{bmatrix} 2 & -\sqrt{6} & -\sqrt{2} \\ -\sqrt{6} & 3 & \sqrt{3} \\ -\sqrt{2} & \sqrt{3} & 1 \end{bmatrix}, \tag{A4}$$

whereas the three molecular orbitals that are odd with respect to the symmetry plane of V^{ortho}, namely, $\{|u_2\rangle, |u_5\rangle, |u_6\rangle\}$, mix under the odd submatrix,

TABLE IV. The numerical factors R_i^x, where $x = o, m, p$, appearing in the residues.

i	R_i^o	R_i^m	R_i^p
1	$N_o^2(1 - 100/9\,\gamma^2 - i\gamma 20/3)$	$N_m^2(1 - 121/36\,\gamma^2 - i\,11/3\,\gamma)$	$N_p^2(1 - 16/9\,\gamma^2 - i8/3\,\gamma)$
2	$N_{o''}^2(1 - 169/36\,\gamma^2 - i\gamma 13/3)$	$N_m^2(1 - 25/36\,\gamma^2 + i\gamma 5/3)$	$N_p^2(1 - 4/9\,\gamma^2 - i4/3\,\gamma)$
3	$N_{o'}^2(1 - 9/4\,\gamma^2 + i\gamma 3)$	$N_{m'}^2(1 - 9/4\,\gamma^2 - i3\gamma)$	
4	$N_{o''}^2(1 - 169/36\,\gamma^2 + i\gamma 13/3)$	$N_m^2(1 - 25/36\,\gamma^2 - i\gamma 5/3)$	$N_p^2(1 - 4/9\,\gamma^2 + i4/3\,\gamma)$
5	$N_{o'}^2(1 - 9/4\,\gamma^2 - i\gamma 3)$	$N_{m'}^2(1 - 9/4\,\gamma^2 + i3\gamma)$	
6	$N_o^2(1 - 100/9\,\gamma^2 + i\gamma 20/3)$	$N_m^2(1 - 121/36\,\gamma^2 + i\,11/3\,\gamma)$	$N_p^2(1 - 16/9\,\gamma^2 + i8/3\,\gamma)$

TABLE V. Meta case. Perturbed eigenvalues and eigenvectors and the residues of the poles of the Green's function.

i	$\varepsilon_i^{(1)}$	Eigenvectors, $\lvert u_i^{(1)}\rangle$	Residue
1	$\alpha+2\beta-i\frac{\Gamma}{6}$	$N_m\left(\lvert u_1\rangle+i\gamma\sqrt{2}\lvert u_2\rangle+i\gamma\frac{\sqrt{2}}{3}\lvert u_4\rangle+i\gamma\frac{1}{2}\lvert u_6\rangle\right)$	$\frac{1}{6}R_1^m$
2	$\alpha+\beta-i\frac{\Gamma}{12}$	$N_m\left(\lvert u_2\rangle-i\gamma\sqrt{2}\lvert u_1\rangle-i\gamma\frac{\sqrt{2}}{3}\lvert u_6\rangle-i\gamma\frac{1}{2}\lvert u_4\rangle\right)$	$\frac{1}{12}R_2^m$
3	$\alpha+\beta-i\frac{\Gamma}{4}$	$N_{m'}\left(\lvert u_3\rangle+i\gamma\frac{3}{2}\lvert u_5\rangle\right)$	$-\frac{1}{4}R_3^m$
4	$\alpha-\beta-i\frac{\Gamma}{12}$	$N_m\left(\lvert u_4\rangle-i\gamma\sqrt{2}\lvert u_6\rangle-i\gamma\frac{\sqrt{2}}{3}\lvert u_1\rangle+i\gamma\frac{1}{2}\lvert u_2\rangle\right)$	$\frac{1}{12}R_4^m$
5	$\alpha-\beta-i\frac{\Gamma}{4}$	$N_{m'}\left(\lvert u_3\rangle-i\gamma\frac{3}{2}\lvert u_5\rangle\right)$	$-\frac{1}{4}R_5^m$
6	$\alpha-2\beta-i\frac{\Gamma}{6}$	$N_m\left(\lvert u_6\rangle+i\gamma\sqrt{2}\lvert u_4\rangle+i\gamma\frac{\sqrt{2}}{3}\lvert u_2\rangle-i\gamma\frac{1}{2}\lvert u_1\rangle\right)$	$\frac{1}{6}R_6^m$

$$V_{\text{odd}}^{o}=-i\frac{\Gamma}{2}\frac{1}{6}\begin{bmatrix}1 & -\sqrt{3} & \sqrt{2}\\ -\sqrt{3} & 3 & -\sqrt{6}\\ \sqrt{2} & -\sqrt{6} & 2\end{bmatrix}. \tag{A5}$$

The perturbed eigenvalues and eigenvectors, to first order in $\gamma=\Gamma/(12\beta)$, are given in Table II. All normalization constants appear in Table III. Also the residues, calculated using Eq. (44), are in the table, and the ortho Green's function, appearing in Eq. (45), can be written out. The numerical factors (R_i^x) appear in Table IV.

In the meta case we also choose the form of the perturbation operator to take advantage of eigenvector symmetry. We have

$$V^{\text{meta}}=-i\frac{\Gamma}{2}(|1\rangle\langle 1|+|3\rangle\langle 3|). \tag{A6}$$

This is rotated to the MO basis, $V^m=U^{-1}V^{\text{meta}}U$. Four eigenvectors are even with respect to the symmetry plane of V^{meta}. In the basis $\{|u_1\rangle,|u_2\rangle,|u_4\rangle,|u_6\rangle\}$ the even submatrix of V^m is given by

$$V_{\text{even}}^{m}=-i\frac{\Gamma}{2}\frac{1}{6}\begin{bmatrix}2 & -\sqrt{2} & -\sqrt{2} & -2\\ -\sqrt{2} & 1 & 1 & \sqrt{2}\\ -\sqrt{2} & 1 & 1 & \sqrt{2}\\ -2 & \sqrt{2} & \sqrt{2} & 2\end{bmatrix}. \tag{A7}$$

Likewise, in the basis $\{|u_3\rangle,|u_5\rangle\}$ the odd submatrix of V^m is given by

$$V_{\text{odd}}^{m}=-i\frac{\Gamma}{2}\frac{1}{6}\begin{bmatrix}3 & -3\\ -3 & 3\end{bmatrix}. \tag{A8}$$

On display in Table V are the perturbed eigenvalues and eigenvectors as well as the residues of the poles of the Green's function.

The simplest case is the para case. The perturbation is chosen to be

TABLE VI. Para case. Perturbed eigenvalues and eigenvectors and the residues of the poles of the Green's function.

i	$\varepsilon_i^{(1)}$	Eigenvectors, $\lvert u_i^{(1)}\rangle$	Residue
1	$\alpha+2\beta-i\Gamma/6$	$N_p(\lvert u_1\rangle-i\gamma 2\sqrt{2}/3\lvert u_4\rangle)$	$1/6R_1^p$
2	$\alpha+\beta-i\Gamma/3$	$N_p(\lvert u_2\rangle+i\gamma 2\sqrt{2}/3\lvert u_6\rangle)$	$-1/3R_2^p$
3	$\alpha+\beta$	$\lvert u_3\rangle$	0
4	$\alpha-\beta-i\Gamma/3$	$N_p(\lvert u_4\rangle+i\gamma 2\sqrt{2}/3\lvert u_1\rangle)$	$1/3R_4^p$
5	$\alpha-\beta$	$\lvert u_5\rangle$	0
6	$\alpha-2\beta-i\Gamma/6$	$N_p(\lvert u_6\rangle-i\gamma 2\sqrt{2}/3\lvert u_2\rangle)$	$-1/6R_6^p$

$$V^{\text{para}}=-i\frac{\Gamma}{2}(|2\rangle\langle 2|+|5\rangle\langle 5|), \tag{A9}$$

and it is rotated to the MO basis, $V^p=U^{-1}V^{\text{para}}U$. The eigenvectors $|u_3\rangle$ and $|u_5\rangle$ have nodes at the sites $|2\rangle$ and $|5\rangle$, so they are not mixed by the perturbation and remain eigenvectors of the full Hamiltonian. Thus the broadened para Green's functions have two poles on the real axis at $\alpha\pm\beta$. Two eigenvectors, $|u_1\rangle$ and $|u_4\rangle$, are even with respect to the symmetry plane of V^{para}. In the basis $\{|u_1\rangle,|u_4\rangle\}$ the even submatrix of V^p is given by

$$V_{\text{even}}^{p}=-i\frac{\Gamma}{2}\frac{1}{6}\begin{bmatrix}2 & 2\sqrt{2}\\ 2\sqrt{2} & 4\end{bmatrix}. \tag{A10}$$

In the basis $\{|u_2\rangle,|u_6\rangle\}$ the odd submatrix of V^p is given by

$$V_{\text{odd}}^{p}=-i\frac{\Gamma}{2}\frac{1}{6}\begin{bmatrix}4 & -2\sqrt{2}\\ -2\sqrt{2} & 2\end{bmatrix}. \tag{A11}$$

The perturbed eigenvalues and eigenvectors and the residues of the poles of the para Green's function are given in Table VI.

[1] G. Engel, T. Calhoun, E. Read, T.-K. Ahn, T. Mancal, Y.-C. Cheng, R. Blankenship, and G. Fleming, Nature (London) **446**, 782 (2007).
[2] H. Lee, Y.-C. Cheng, and G. R. Fleming, Science **316**, 1462 (2007).
[3] R. Baer and D. Neuhauser, J. Am. Chem. Soc. **124**, 4200 (2002).
[4] R. Baer and D. Neuhauser, Chem. Phys. **281**, 353 (2002).
[5] D. M. Cardamone, C. A. Stafford, and S. Mazumdar, Nano Lett. **6**, 2422 (2006).
[6] R. Stadler, M. Forshaw, and C. Joachim, Nanotechnology **14**, 138 (2003).
[7] R. Stadler, S. Ami, C. Joachim, and M. Forshaw, Nanotechnology **15**, S115 (2004).
[8] D. Q. Andrews, G. C. Solomon, R. P. Van Duyne, and M. A. Ratner, J. Am. Chem. Soc. **130**, 17309 (2008).
[9] D. Xiao, S. S. Skourtis, I. V. Rubtsov, and D. N. Beratan, Nano Lett. **9**, 1818 (2009).
[10] P. R. Levstein, H. M. Pastawski, and J. L. D'Amato, J. Phys.: Condens. Matter **2**, 1781 (1990).
[11] E. G. Emberly and G. Kirczenow, J. Phys.: Condens. Matter **11**, 6911 (1999).
[12] H. W. Lee, Phys. Rev. Lett. **82**, 2358 (1999).
[13] C. Kalyanaraman and D. Evans, Nano Lett. **2**, 437 (2002).
[14] R. Collepardo-Guevara, D. Walter, D. Neuhauser, and R. Baer, Chem. Phys. Lett. **393**, 367 (2004).
[15] M. Ernzerhof, M. Zuang, and P. Rocheleau, J. Chem. Phys. **123**, 134704 (2005).
[16] D. Brisker, I. Cherkes, C. Gnodtke, D. Jarukanont, S. Klaiman, W. Koch, S. Weissman, R. Volkovich, M. Toroker, and U. Peskin, Mol. Phys. **106**, 281 (2008).
[17] G. C. Solomon, D. Q. Andrews, R. H. Goldsmith, T. Hansen, M. R. Wasielewski, R. P. Van Duyne, and M. A. Ratner, J. Am. Chem. Soc. **130**, 17301 (2008).

[18] G. C. Solomon, D. Q. Andrews, T. Hansen, R. H. Goldsmith, M. R. Wasielewski, R. P. Van Duyne, and M. A. Ratner, J. Chem. Phys. **129**, 054701 (2008).
[19] D. Q. Andrews, G. C. Solomon, R. H. Goldsmith, T. Hansen, M. R. Wasielewski, R. P. V. Duyne, and M. A. Ratner, J. Phys. Chem. C **112**, 16991 (2008).
[20] G. C. Solomon, D. Q. Andrews, R. P. Van Duyne, and M. A. Ratner, J. Am. Chem. Soc. **130**, 7788 (2008).
[21] G. C. Solomon, D. Q. Andrews, R. P. V. Duyne, and M. A. Ratner, ChemPhysChem **10**, 257 (2009).
[22] B. Pickup and P. Fowler, Chem. Phys. Lett. **459**, 198 (2008).
[23] P. Fowler, B. Pickup, and T. Todorova, Chem. Phys. Lett. **465**, 142 (2008).
[24] P. W. Fowler, B. T. Pickup, T. Z. Todorova, and T. Pisanski, J. Chem. Phys. **130**, 174708 (2009).
[25] L.-Y. Hsu and B.-Y. Jin, Chem. Phys. **355**, 177 (2009).
[26] C. Patoux, C. Coudret, J. P. Launay, C. Joachim, and A. Gourdon, Inorg. Chem. **36**, 5037 (1997).
[27] M. Mayor, H. Weber, J. Reichert, M. Elbing, C. von Hänisch, D. Beckmann, and M. Fischer, Angew. Chem., Int. Ed. **42**, 5834 (2003).
[28] P. Sautet and C. Joachim, Chem. Phys. Lett. **153**, 511 (1988).
[29] P. Sautet and C. Joachim, Chem. Phys. **135**, 99 (1989).
[30] C. Joachim, J. Gimzewski, and H. Tang, Phys. Rev. B **58**, 16407 (1998).
[31] S. Yaliraki and M. Ratner, Ann. N.Y. Acad. Sci. **960**, 153 (2002).
[32] D. Walter, D. Neuhauser, and R. Baer, Chem. Phys. **299**, 139 (2004).
[33] M. Ernzerhof, H. Bahmann, F. Goyer, M. Zuang, and P. Rocheleau, J. Chem. Theory Comput. **2**, 1291 (2006).
[34] T. A. Papadopoulos, I. M. Grace, and C. J. Lambert, Phys. Rev. B **74**, 193306 (2006).
[35] S. K. Maiti, Chem. Phys. **331**, 254 (2007).
[36] K. Yoshizawa, T. Tada, and A. Staykov, J. Am. Chem. Soc. **130**, 9406 (2008).
[37] S.-H. Ke, W. Yang, and H. U. Baranger, Nano Lett. **8**, 3257 (2008).
[38] D. Darau, G. Begemann, A. Donarini, and M. Grifoni, Phys. Rev. B **79**, 235404 (2009).
[39] M. A. Ratner, J. Phys. Chem. **94**, 4877 (1990).
[40] S. S. Skourtis and D. N. Beratan, *Theories of Structure-Function Relationship for Bridge-Mediated Electron Transfer*, Advances in Chemical Physics, Vol. 106 (Wiley, New York, 1999), Chap. 8, pp. 377–452.
[41] C. Goldman, Phys. Rev. A **43**, 4500 (1991).
[42] Y. Magarshak, J. Malinsky, and A. D. Joran, J. Chem. Phys. **95**, 418 (1991).
[43] O. L. de Santana and A. A. S. da Gama, Chem. Phys. Lett. **314**, 508 (1999).
[44] S. Datta, *Quantum Transport: Atom to Transistor* (Cambridge University Press, Cambridge, 2005).
[45] S. Datta, Phys. Rev. B **40**, 5830 (1989).
[46] Y. Meir and N. S. Wingreen, Phys. Rev. Lett. **68**, 2512 (1992).
[47] W. Tian, S. Datta, S. Hong, R. Reifenberger, J. I. Henderson, and C. P. Kubiak, J. Chem. Phys. **109**, 2874 (1998).
[48] M. P. Samanta, W. Tian, S. Datta, J. I. Henderson, and C. P. Kubiak, Phys. Rev. B **53**, R7626 (1996).
[49] L. E. Hall, J. R. Reimers, N. S. Hush, and K. Silverbrook, J. Chem. Phys. **112**, 1510 (2000).
[50] J. Taylor, H. Guo, and J. Wang, Phys. Rev. B **63**, 245407 (2001).
[51] M. Brandbyge, J.-L. Mozos, P. Ordejon, J. Taylor, and K. Stokbro, Phys. Rev. B **65**, 165401 (2002).
[52] Y. Xue, S. Datta, and M. A. Ratner, Chem. Phys. **281**, 151 (2002).
[53] D. S. Fisher and P. A. Lee, Phys. Rev. B **23**, 6851 (1981).
[54] T. N. Todorov, J. Phys.: Condens. Matter **14**, 3049 (2002).
[55] P. Lancaster and M. Tismenetsky, *The Theory of Matrices*, 2nd ed. (Academic, San Diego, 1985).
[56] P.-O. Löwdin, J. Math. Phys. **3**, 969 (1962).
[57] C. Cohen-Tannoudji, J. Dupont-Roc, and G. Grynberg, *Atom-Photon Interactions* (Wiley, New York, 1992).
[58] A. Messiah, *Quantum Mechanics* (Dover, Mineola, 1999).
[59] P. W. Anderson, Phys. Rev. **109**, 1492 (1958).
[60] E. Economou, *Green's Functions in Quantum Physics*, 3rd ed. (Springer, New York, 2006).
[61] E. V. Anslyn and D. A. Dougherty, *Modern Physical Organic Chemistry* (University Science Books, Sausalito, 2005).
[62] C. Coulson and G. Rushbrooke, Proc. Cambridge Philos. Soc. **36**, 193 (1940).
[63] N. Trinajstic, *Chemical Graph Theory*, 2nd ed. (CRC, Boca Raton, 1992).